Semi-algebraic mode analysis for finite element discretisations of the heat equation

Noora Habibi[*]
Faculty of Applied Mathematics, Shahrood University Of Technology,
P.O. Box 3619995161, Shahrood, Iran.
E-mail: habibi85nu@gmail.com

Ali Mesforoush
Faculty of Applied Mathematics, Shahrood University Of Technology,
P.O. Box 3619995161, Shahrood, Iran.
E-mail: ali.mesforush@shahroodut.ac.ir

Francisco J. Gaspar Lorenz
Department of Applied Mathematics, Science Faculty, University of Zaragoza,
Pedro Cerbuna, 12, 50009 Zaragoza, Spain.
E-mail: fjgaspar@unizar.es

Carmen Rodrigo
Department of Applied Mathematics, School of Engineering and Architecture,
University of Zaragoza, Maria de Luna, 3, 50018, Zaragoza, Spain.
E-mail: carmenr@unizar.es

Abstract	In this work, a semialgebraic mode analysis (SAMA) is proposed for investigating the convergence of a multigrid waveform relaxation method applied to the Finite Element (FE) discretization of the heat equation in two and three dimensions. This analysis for finite element methods is more involved and more general than that for Finite Difference (FD) discretizations, since mass matrix must be considered. The proposed analysis results in a very useful tool to study the behaviour of the multigrid waveform relaxation method depending on the parameters of the problem.

1. Introduction

The Semi-Algebraic Mode Analysis (SAMA) was introduced by Friedhoff and MacLachlan in [3] for predicting the convergence factor of time-dependent Partial Differential Equations (PDEs) as a generalization of Local Fourier Analysis (LFA). LFA is the most powerful technique for predicting the convergence of multigrids methods [10, 12]. This method analyzes the behavior of the local components involved in multigrid methods on a basis of complex exponential functions. LFA, however, has not been successful in predicting the convergence factor for time dependent PDE

problems [1, 3], and to overcome this failure, SAMA was introduced. The main idea of SAMA is the combination of LFA only in space with an exact analytical approach in time. In this work, we utilize SAMA to analyze the convergence factor of multigrid waveform relaxation applied to finite element discretization of the heat equation.

Let us consider as model problem the heat equation with homogeneous Dirichlet boundary conditions

$$
\begin{aligned}
& D_t u(\mathbf{x}, t) - \Delta u(\mathbf{x}, t)) = f(\mathbf{x}, t), \quad \mathbf{x} \in \Omega, \quad t > 0, \\
& u(\mathbf{x}, t) = 0, \quad \text{on } \partial\Omega, \quad t > 0, \\
& u(\mathbf{x}, 0) = g(\mathbf{x}), \quad \mathbf{x} \in \Omega,
\end{aligned}
\tag{1.1}
$$

where $\Omega \subset \mathbb{R}^d$, for $d = 2$ (or $d = 3$) is a bounded domain with boundary $\partial\Omega$. In order to establish the finite element approximation of our problem, let Ω_h be a triangulation of Ω, satisfying the usual admissibility assumption, i.e. the intersections of two different elements is either empty, a vertex, or a whole edge. Let V_h be the finite element space of continuous piecewise bilinear (or trilinear) functions associated with Ω_h vanishing on the boundary $\partial\Omega$. The discrete approximation $u_h \in V_h$ solves the following problem

$$
(D_t u_h, v_h) + a(u_h, v_h) = (f, v_h) \quad v_h \in V_h,
$$

where

$$
(D_t u_h, v_h) = \int_\Omega (D_t u_h) v_h \, d\mathbf{x}, \qquad (f, v_h) = \int_\Omega f v_h \, d\mathbf{x}
$$

$$
a(u_h, v_h) = \int_\Omega \nabla u_h \cdot \nabla v_h \, d\mathbf{x}.
$$

Let $\{\phi_1, \ldots, \phi_N\}$ be the nodal basis of V_h, i.e., $\phi_i(\mathbf{x}_j) = \delta_{ij}$, with $\mathbf{x}_j$ an interior node of the mesh Ω_h. The approximation $u_h = \sum_{i=1}^N u_i(t)\phi_i(\mathbf{x})$ is found by solving the following set of equations,

$$
(D_t u_h, \phi_j) + a(u_h, \phi_j) = (f, \phi_j), \quad \text{for } j = 1, 2, \ldots, N.
$$

We rewrite these equations in terms of the mass matrix $B = \{(\phi_i, \phi_j)\}$ and the stiffness matrix $A = \{a(\phi_i, \phi_j)\}$, in a more standard form, as a system of ordinary differential equations (ODEs)

$$
B_h \dot{\mathbf{u}}_h(t) + A_h \mathbf{u}_h(t) = F_h(t), \quad \mathbf{u}_h(0) = g_h, \quad t > 0,
\tag{1.2}
$$

where $\mathbf{u}_h(t) = [u_1(t), u_2(t), \ldots, u_N(t)]^t \in \mathbb{R}^N$ and the coefficient matrices $A_h, B_h \in \mathbb{R}^{N \times N}$ and the right hand side $F_h(t) = [(f, \phi_1), (f, \phi_2), \ldots, (f, \phi_N)]^T \in \mathbb{R}^N$ are considered.

We have many choices to pick a suitable method for solving the obtained ODE system (1.2). In general, we can divide all the well known methods into two classes: time-marching approaches and time parallel techniques. In a time marching approach, we solve in each time step a time-independent problem then we go to the next time step. Indeed, as we can get out from its name, each time step will be solved after the other in a sequential manner, see Figure 1 (left). Although this approach is simpler, when we need multiprocessing capability or parallelization of the temporal

FIGURE 1. Time-stepping (at left) versus waveform relaxation (at right). In this figure ν_i, for $i = 1, 2, \ldots$ indicates to the iterations of two methods.
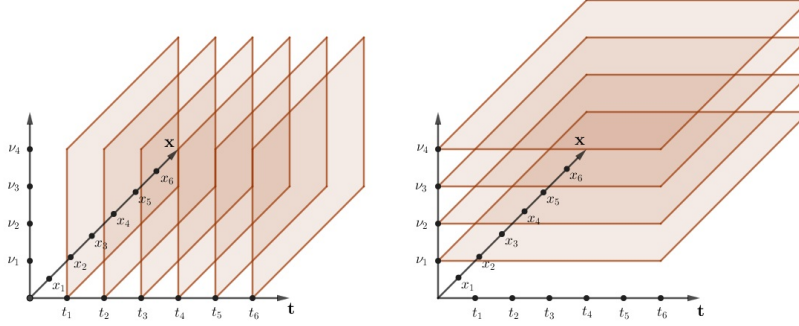
variable we have to seek for another approach. So we consider a full space-time method. The time parallel class itself can be classified into four groups of methods (see [5]): Multiple shooting; Domain decomposition and waveform relaxation; Space-time multigrid method; and Direct time parallel methods. Here, we only concentrate on the waveform relaxation method and in particular, on its multigrid extension.

The waveform relaxation method (WR) is a technique for solving ordinary differential equations. It can be also applied to time-dependent PDEs when their spatial derivatives are replaced by a discrete formula (obtained by the Finite Element method in our particular case) as viewpoint of the method of lines scheme. The WR method is based on splitting matrices A_h and B_h as $B_h = M_{B_h} - N_{B_h}$ and $A_h = M_{A_h} - N_{A_h}$, leading to the following iteration

$$M_{B_h} \dot{\mathbf{u}}_h^k(t) + M_{A_h} \mathbf{u}_h^k(t) = N_{B_h} \dot{\mathbf{u}}_h^{k-1}(t) + N_{A_h} \mathbf{u}_h^{k-1}(t) + F_h(t), \qquad (1.3)$$

where $\mathbf{u}_h^k(0) = g_h$, for $k \geq 1$ and $\mathbf{u}_h^k(t)$ indicates the approximation of $\mathbf{u}(t)$ at iteration k. It is natural to define $\mathbf{u}_h^0(t)$ along the whole time interval equal to the initial condition, i.e. $\mathbf{u}_h^0(t) = g_h$, $t > 0$. Considering the decomposition of matrices A_h and B_h as $A_h = -L_{A_h} + D_{A_h} - U_{A_h}$ and $B_h = -L_{B_h} + D_{B_h} - U_{B_h}$, where L_{A_h} and L_{B_h} are strictly lower triangular matrices, D_{A_h} and D_{B_h} are diagonal matrices, and U_{A_h} and U_{B_h} are strictly upper triangular matrices, for the Gauss-Seidel waveform relaxation method, which is considered in this work, the splittings in (1.3) are as follows:

$$M_{A_h} = -L_{A_h} + D_{A_h} \quad N_{A_h} = U_{A_h},$$
$$M_{B_h} = -L_{B_h} + D_{B_h} \quad N_{B_h} = U_{B_h}.$$

We use multigrid technique to accelerate the convergence of the Gauss-Seidel waveform relaxation method. A multigrid acceleration of this method was firstly studied by Lubich and Ostermann in [9] and independently developed in [11].

In order to apply a geometric multigrid waveform relaxation procedure the coarsening applies only in the spatial domain and we consider a hierarchy of grids like

$\Omega_{2^l h} \subset \ldots \subset \Omega_{2h} \subset \Omega_h$. We obtain a new iterate $\mathbf{u}_h^{(k)}$ from the former waveform $\mathbf{u}_h^{(k-1)}$ in three steps: Pre-smoothing, coarse grid correction and post smoothing. In Algorithm 1 we present the multigrid waveform relaxation algorithm (WRMG) depending on the defined Gauss-Seidel waveform relaxation method as smoother and the rest of the operators involved in the multigrid procedure. We consider standard coarsening for constructing the coarse meshes and discretization coarse grid approximation (DCA) in coarser grids. Regarding intergrid transfer operators, the interpolation operators are the nine point stencil operator corresponding to the bilinear interpolation for two dimensional problems and its generalization for three dimensional problems, that is, the trilinear interpolation operator. The restriction operators are considered as the adjoint of the prolongation operators.

Algorithm 1 Multigrid waveform relaxation based on Gauss-Seidel smoother $\mathbf{u}_h^{(k)}(t) \rightarrow \mathbf{u}_h^{(k+1)}(t)$

If we are on the coarsest grid (given by spatial grid size $2^l h = h_0$), then solve the following equation by a direct or fast solver

$\qquad B_{h_0} \dot{\mathbf{u}}_{h_0}^{k+1}(t) + A_{h_0} \mathbf{u}_{h_0}^{k+1}(t) = F_{h_0}(t).$

Else

(*Presmoothing*) Perform k_1 steps of Gauss-Seidel waveform relaxation,

$\qquad v_h^k(t) = S^{k_1}\left(\mathbf{u}_h^k(t)\right).$

(*Coarse grid correction*)

$\qquad$ Compute the defect

$\qquad \bar{d}_h^k(t) = F_h(t) - B_h \dot{v}_h^k(t) - A_h v_h^k(t)$

$\qquad$ Restrict the defect

$\qquad \bar{d}_{2h}^k(t) = I_h^{2h} \bar{d}_h^k(t)$

$\qquad$ Perform $\gamma \geq 1$ cycles of WRMG on Ω_{2h} to solve the following defect equation,

$\qquad B_{2h} \dot{e}_{2h}^k(t) + A_{2h} e_{2h}^k(t) = \bar{d}_{2h}^k(t), \ e_{2h}^k(0) = 0$

$\qquad$ Interpolate the correction

$\qquad e_h^k(t) = I_{2h}^h e_{2h}^k(t)$

$\qquad$ Correct the current approximation with the interpolation of the correction,

$\qquad v_h^{k+1}(t) = v_h^k(t) + e_h^k(t).$

(*Postsmoothing*) Perform k_2 steps of Gauss-Seidel waveform relaxation,

$\qquad \mathbf{u}_h^{k+1}(t) = S^{k_2}\left(v_h^{k+1}(t)\right).$

End If

In Algorithm 1, using the Crank-Nicolson approach for time discretization we obtain a space-time multigrid method with coarsening only in space. Thus, we have time-line Gauss-Seidel waveform relaxation, with standard full weighting restriction and bilinear interpolation in space for data transfer between the levels in the multigrid hierarchy.

In the rest of this work, first we explain the two-grid SAMA analysis in two dimensions for Gauss-Seidel waveform relaxation with multigrid acceleration in Section 2.1. At the end of this section, Section 2.2, we will present our analysis for the considered model problem (1.2), by defining all required stencils involved in the FE method with bilinear basis functions. Section 3 is devoted to extending SAMA analysis to three

dimensions. Again, at the end of Section 3 we perform some analysis for our particular model problem introducing all necessary stencils for the FE method with trilinear basis functions. Conclusions are drawn in Section 4.

2. SAMA in two dimensions

2.1. **Theoretical framework.** Now, we describe the convergence analysis of the multigrid waveform relaxation method by SAMA. For this end, we will do the following steps.

(1) First, we present some primary definitions,
(2) Next, we explain SAMA smoothing analysis for the Gauss-Seidel relaxation procedure,
(3) Then, we investigate the analysis for the coarse-grid correction operator,
(4) Finally, we combine the two last steps to perform a complete two-grid analysis.

We define the infinite grid $\mathcal{Q}_h = \{\mathbf{x} = \mathbf{k}\mathbf{h} = (k_1 h_1, k_2 h_2), \ \mathbf{k} \in \mathbb{Z}^2\}$, and the so-called Fourier modes as $\varphi_h(\boldsymbol{\theta}, \mathbf{x}) = e^{i\boldsymbol{\theta} \cdot \mathbf{x}} = e^{i\theta_1 x_1} e^{\theta_2 x_2}$ where $\mathbf{h}$ is the spatial discretization step and $\boldsymbol{\theta} \in \Theta_h = (-\pi/h, \pi/h]^2$. Now, we can define any discrete grid function for a fixed t as a formal linear combination of the Fourier modes by

$$u_h(\mathbf{x}, t) = \sum_{\boldsymbol{\theta} \in \Theta_h} c_{\boldsymbol{\theta}}(t) \varphi_h(\boldsymbol{\theta}, \mathbf{x}), \quad \mathbf{x} \in \mathcal{Q}_h, \tag{2.1}$$

where coefficients $c_{\boldsymbol{\theta}}(t)$ depend on the time variable. The Fourier modes yield the so-called Fourier space $\mathcal{F}(\mathcal{Q}_h) = \{\varphi_h(\boldsymbol{\theta}, \mathbf{x}), \boldsymbol{\theta} \in \Theta_h\}$, and they are formal eigenfunctions of any discrete operator L_h, e.g. for the standard discrete Laplace operator, $L_h = -\Delta_h = \frac{1}{h^2}[-1 \ 2 \ -1]$, the expression $L_h \varphi_h(\boldsymbol{\theta}, \mathbf{x}) = \widehat{L}_h(\boldsymbol{\theta}) \varphi_h(\boldsymbol{\theta}, \mathbf{x})$ holds where

$$\widehat{L}_h(\boldsymbol{\theta}) = \frac{2}{h^2} \left(1 - \cos(\theta h)\right),$$

is the Fourier representation of L_h on the Fourier space, also called formal eigenvalue or the Fourier symbol of L_h.

Now, we study the effect of Gauss-Seidel relaxation procedure and the coarse-grid correction operator on the Fourier modes. To reach this goal, we need to define the high- and low-frequency components with respect to the coarsening strategy. We consider $\Theta_{2h} = (-\pi/2h, \pi/2h]^2$ and $\Theta_h \smallsetminus \Theta_{2h}$ as the low- and high frequency spaces, respectively. Here, we have used the standard coarsening which means that the step size is double on the coarse grid, denoted by $\mathcal{Q}_{2h}$.

By considering $A_h = M_{A_h} - N_{A_h}$ and $B_h = M_{B_h} - N_{B_h}$ that have been defined in the previous section, we can write an iteration of the waveform relaxation method for an error grid function as:

$$M_{B_h} \dot{e}_h^k(\mathbf{x}, t) + M_{A_h} e_h^k(\mathbf{x}, t) = N_{B_h} \dot{e}_h^{k-1}(\mathbf{x}, t) + N_{A_h} e_h^{k-1}(\mathbf{x}, t), \tag{2.2}$$

for $k \geq 1$, $\mathbf{x} \in \mathcal{Q}_h$ and $t > 0$, where, $e_h^{k-1}(\cdot, t)$ and $e_h^k(\cdot, t)$ are the error grid functions at the $k-1$ and k iterations and $e_h^k(\mathbf{x}, 0) = 0$.

Following equation (2.1), we can write $e_h^i(\mathbf{x}, t)$ in the ith iteration as:

$$e_h^i(\mathbf{x}, t) = \sum_{\boldsymbol{\theta} \in \Theta_h} c_{\boldsymbol{\theta}}^i(t) \varphi_h(\boldsymbol{\theta}, \mathbf{x}), \quad \mathbf{x} \in \mathcal{Q}_h, \ t > 0. \tag{2.3}$$

We denote as $\widehat{M}_{A_h}(\boldsymbol{\theta})$, $\widehat{M}_{B_h}(\boldsymbol{\theta})$, $\widehat{N}_{A_h}(\boldsymbol{\theta})$ and $\widehat{N}_{B_h}(\boldsymbol{\theta})$ the symbols of M_{A_h}, M_{B_h}, N_{A_h} and N_{B_h}, respectively. So, for each frequency $\boldsymbol{\theta} \in \Theta_h$ we have

$$\widehat{M}_{B_h}(\boldsymbol{\theta})\dot{c}_{\boldsymbol{\theta}}^k(t) + \widehat{M}_{A_h}(\boldsymbol{\theta})c_{\boldsymbol{\theta}}^k(t) = \widehat{N}_{B_h}(\boldsymbol{\theta})\dot{c}_{\boldsymbol{\theta}}^{k-1}(t) + \widehat{N}_{A_h}(\boldsymbol{\theta})c_{\boldsymbol{\theta}}^{k-1}(t), \tag{2.4}$$

for $k \geq 1$, $t > 0$. Considering a uniform grid in time with M subdivisions and time step size τ, we apply the Crank-Nicolson time discretization on equation (2.4), given by

$$\widehat{M}_{B_h}(\boldsymbol{\theta}) \frac{c_{\boldsymbol{\theta},i}^k - c_{\boldsymbol{\theta},i-1}^k}{\tau} - \widehat{N}_{B_h}(\boldsymbol{\theta}) \frac{c_{\boldsymbol{\theta},i}^{k-1} - c_{\boldsymbol{\theta},i-1}^{k-1}}{\tau}$$
$$= \frac{1}{2}\left(-\widehat{M}_{A_h}(\boldsymbol{\theta})c_{\boldsymbol{\theta},i}^k + \widehat{N}_{A_h}(\boldsymbol{\theta})c_{\boldsymbol{\theta},i}^{k-1}\right) + \frac{1}{2}\left(-\widehat{M}_{A_h}(\boldsymbol{\theta})c_{\boldsymbol{\theta},i-1}^k + \widehat{N}_{A_h}(\boldsymbol{\theta})c_{\boldsymbol{\theta},i-1}^{k-1}\right). \tag{2.5}$$

Denoting by $(c_{\boldsymbol{\theta},1}^k, c_{\boldsymbol{\theta},2}^k, \ldots, c_{\boldsymbol{\theta},M}^k)$ the approximation of $c_{\boldsymbol{\theta}}^k(t)$ on the defined uniform grid in time, we obtain the following matrix form

$$\begin{pmatrix} c_{\boldsymbol{\theta},1}^k \\ c_{\boldsymbol{\theta},2}^k \\ \vdots \\ c_{\boldsymbol{\theta},M}^k \end{pmatrix} = \widetilde{\mathcal{M}}_{h,\tau}^{-1}(\boldsymbol{\theta}) \widetilde{\mathcal{N}}_{h,\tau}(\boldsymbol{\theta}) \begin{pmatrix} c_{\boldsymbol{\theta},1}^{k-1} \\ c_{\boldsymbol{\theta},2}^{k-1} \\ \vdots \\ c_{\boldsymbol{\theta},M}^{k-1} \end{pmatrix},$$

where

$$\widetilde{\mathcal{M}}_{h,\tau}(\boldsymbol{\theta}) =$$
$$\begin{pmatrix} \frac{1}{\tau}\widehat{M}_{B_h}(\boldsymbol{\theta})+\frac{1}{2}\widehat{M}_{A_h}(\boldsymbol{\theta}) & 0 & \cdots & 0 \\ -\frac{1}{\tau}\widehat{M}_{B_h}(\boldsymbol{\theta})+\frac{1}{2}\widehat{M}_{A_h}(\boldsymbol{\theta}) & \frac{1}{\tau}\widehat{M}_{B_h}(\boldsymbol{\theta})+\frac{1}{2}\widehat{M}_{A_h}(\boldsymbol{\theta}) & \cdots & 0 \\ \vdots & \ddots & \ddots & \vdots \\ 0 & \cdots & -\frac{1}{\tau}\widehat{M}_{B_h}(\boldsymbol{\theta})+\frac{1}{2}\widehat{M}_{A_h}(\boldsymbol{\theta}) & \frac{1}{\tau}\widehat{M}_{B_h}(\boldsymbol{\theta})+\frac{1}{2}\widehat{M}_{A_h}(\boldsymbol{\theta}) \end{pmatrix}.$$

We can obtain $\widetilde{\mathcal{N}}_{h,\tau}(\boldsymbol{\theta})$ as $\widetilde{\mathcal{M}}_{h,\tau}(\boldsymbol{\theta})$ by only substituting $\widehat{M}(\boldsymbol{\theta})$ with $\widehat{N}(\boldsymbol{\theta})$ in the above matrix. We can immediately define the smoothing factor of the Gauss-Seidel relaxation operator by considering its symbol $\widetilde{\mathcal{S}}_{h,\tau}(\boldsymbol{\theta}) = \widetilde{\mathcal{M}}_{h,\tau}^{-1}(\boldsymbol{\theta})\widetilde{\mathcal{N}}_{h,\tau}(\boldsymbol{\theta})$, that is

$$\mu = \sup_{\Theta_h \smallsetminus \Theta_{2h}} \left(\rho\left(\widetilde{\mathcal{S}}_{h,\tau}(\boldsymbol{\theta})\right) \right). \tag{2.6}$$

Now, we present the analysis of the coarse-grid correction method. As before, we investigate the effect of the coarse-grid correction, C_h^{2h}, on the Fourier modes. The coarse-grid correction operator is given by:

$$C_h^{2h} = I_h - I_{2h}^h (B_{2h}D_t + \Sigma_t A_{2h})^{-1} I_h^{2h}(B_h D_t + \Sigma_t A_h), \tag{2.7}$$

where D_t and Σ_t are operators corresponding to the Crank-Nicolson approach and I_h, I_{2h}^h, I_h^{2h} are the identity operator, the transfer operator from coarse to fine grids and vice versa. Also, $(B_{2h}D_t + \Sigma_t A_{2h})$ and $(B_h D_t + \Sigma_t A_h)$ are the coarse- and fine-grid operators, respectively.

Our analysis has to take into account the fact that some of the Fourier modes $\varphi_h(\boldsymbol{\theta}, \cdot)$ on the fine grid coincide on $\mathcal{Q}_{2h}$. For any low frequency $\boldsymbol{\theta}^{00} = (\theta_1, \theta_2) \in \Theta_{2h}$, we consider the frequencies $\boldsymbol{\theta}^\alpha = \boldsymbol{\theta}^{00} - (\alpha_1 \text{sign}(\theta_1), \alpha_2 \text{sign}(\theta_2))\frac{\pi}{h}$, where $\alpha = \{(\alpha_1, \alpha_2)|\alpha_j \in \{0,1\}, j = 1, 2\}$. The corresponding four Fourier modes $\varphi_h(\boldsymbol{\theta}^\alpha, \cdot)$ are called harmonics of each other and they form the space of $2h-$ harmonics for $\boldsymbol{\theta} = \boldsymbol{\theta}^{00} \in \Theta_{2h}$, as follows

$$\mathcal{F}_{2h}(\boldsymbol{\theta}) = \text{span}\{\varphi_h(\boldsymbol{\theta}^{00}, \cdot), \varphi_h(\boldsymbol{\theta}^{11}, \cdot), \varphi_h(\boldsymbol{\theta}^{10}, \cdot), \varphi_h(\boldsymbol{\theta}^{01}, \cdot)\}.$$

The space of $2h-$harmonics is invariant under the coarse-grid correction operator. Then, the representation of C_h^{2h} on the space $\mathcal{F}_{2h}$ is a 4×4 matrix $\widehat{C}_h^{2h}(\boldsymbol{\theta})$. To be more precise, we define two vectors: $\boldsymbol{\varphi}_h(\boldsymbol{\theta}, \cdot) = (\varphi_h(\boldsymbol{\theta}^{00}, \cdot), \varphi_h(\boldsymbol{\theta}^{11}, \cdot), \varphi_h(\boldsymbol{\theta}^{10}, \cdot), \varphi_h(\boldsymbol{\theta}^{01}, \cdot))$ and $\mathbf{c}_{\boldsymbol{\theta}}^k(t) = (c_{\boldsymbol{\theta}^{00}}^k(t), c_{\boldsymbol{\theta}^{11}}^k(t), c_{\boldsymbol{\theta}^{10}}^k(t), c_{\boldsymbol{\theta}^{01}}^k(t))$, and then, the error at the k-th iteration will be $e_h^k(\mathbf{x}, t) = \sum_{\boldsymbol{\theta} \in \Theta_{2h}} \mathbf{c}_{\boldsymbol{\theta}}^k(t) \, \boldsymbol{\varphi}_h(\boldsymbol{\theta}, \mathbf{x})^T$. After applying the coarse-grid correction operator on this error, we obtain $\sum_{\boldsymbol{\theta} \in \Theta_{2h}} \widehat{C}_h^{2h}(\boldsymbol{\theta})\mathbf{c}_{\boldsymbol{\theta}}^k(t) \cdot \boldsymbol{\varphi}_h(\boldsymbol{\theta}, \cdot)$, where $\widehat{C}_h^{2h}(\boldsymbol{\theta})$ is the following 4×4 matrix

$$\widehat{C}_h^{2h}(\boldsymbol{\theta}) = I_4 - \widehat{I}_{2h}^h(\boldsymbol{\theta})(\widehat{B}_{2h}(\boldsymbol{\theta})D_t + \Sigma_t \widehat{A}_{2h}(\boldsymbol{\theta}))^{-1}\widehat{I}_h^{2h}(\widehat{B}_h(\boldsymbol{\theta})D_t + \Sigma_t \widehat{A}_h(\boldsymbol{\theta})),$$

where, I_4 is the 4×4 identity matrix, $\widehat{A}_{2h}(\boldsymbol{\theta})$ and $\widehat{B}_{2h}(\boldsymbol{\theta})$ are 1×1 symbols of the discrete operators on the coarse grid, and the rest of the involved Fourier symbols are given by:

$\widehat{A}_h(\boldsymbol{\theta}) = diag\left(\widehat{A}_h(\boldsymbol{\theta}^{00}), \widehat{A}_h(\boldsymbol{\theta}^{11}), \widehat{A}_h(\boldsymbol{\theta}^{10}), \widehat{A}_h(\boldsymbol{\theta}^{01})\right),$

$\widehat{B}_h(\boldsymbol{\theta}) = diag\left(\widehat{B}_h(\boldsymbol{\theta}^{00}), \widehat{B}_h(\boldsymbol{\theta}^{11}), \widehat{B}_h(\boldsymbol{\theta}^{10}), \widehat{B}_h(\boldsymbol{\theta}^{01})\right),$

$\widehat{I}_{2h}^h(\boldsymbol{\theta}) = \left(\widehat{I}_{2h}^h(\boldsymbol{\theta}^{00}), \widehat{I}_{2h}^h(\boldsymbol{\theta}^{11}), \widehat{I}_{2h}^h(\boldsymbol{\theta}^{10}), \widehat{I}_{2h}^h(\boldsymbol{\theta}^{01})\right)^T,$

$\widehat{I}_h^{2h}(\boldsymbol{\theta}) = \left(\widehat{I}_h^{2h}(\boldsymbol{\theta}^{00}), \widehat{I}_h^{2h}(\boldsymbol{\theta}^{11}), \widehat{I}_h^{2h}(\boldsymbol{\theta}^{10}), \widehat{I}_h^{2h}(\boldsymbol{\theta}^{01})\right).$

Now, by considering the time discretization of operators D_t and Σ_t, we obtain the following $M \times M$ matrices:

$$D_t = \frac{1}{\tau}\begin{pmatrix} 1 & 0 & \cdots & 0 \\ -1 & 1 & \cdots & 0 \\ \vdots & \ddots & \ddots & \vdots \\ 0 & \cdots & -1 & 1 \end{pmatrix}, \quad \Sigma_t = \frac{1}{2}\begin{pmatrix} 1 & 0 & \cdots & 0 \\ 1 & 1 & \cdots & 0 \\ \vdots & \ddots & \ddots & \vdots \\ 0 & \cdots & 1 & 1 \end{pmatrix},$$

Thus, the error after application of the coarse grid correction is given by $\widetilde{\mathcal{C}}_{h,\tau}^{2h}(\boldsymbol{\theta})\mathbf{c}_{\boldsymbol{\theta}}^k(t) \cdot \boldsymbol{\varphi}_h(\boldsymbol{\theta}, \cdot)^T$, where the $4M \times 4M$ matrix $\widetilde{\mathcal{C}}_{h,\tau}^{2h}(\boldsymbol{\theta})$ is:

$$\widetilde{\mathcal{C}}_{h,\tau}^{2h}(\boldsymbol{\theta}) = I_{4M} - \widetilde{\mathcal{I}}_{2h}^h(\boldsymbol{\theta})\left(\widetilde{\mathcal{K}}_{2h,\tau}(\boldsymbol{\theta})\right)^{-1}\widetilde{\mathcal{I}}_h^{2h}(\boldsymbol{\theta})\widetilde{\mathcal{K}}_{h,\tau}(\boldsymbol{\theta}),$$

such that I_{4M} is the identity matrix of order $4M$ and $\widetilde{\mathcal{K}}_{h,\tau}(\boldsymbol{\theta})$ is a $4M \times 4M$ matrix defined as:

$$\widetilde{\mathcal{K}}_{h,\tau}(\boldsymbol{\theta}) = \begin{pmatrix} \widetilde{\mathcal{K}}_{h,\tau}(\boldsymbol{\theta}^{00}) & 0 & 0 & 0 \\ 0 & \widetilde{\mathcal{K}}_{h,\tau}(\boldsymbol{\theta}^{11}) & 0 & 0 \\ 0 & 0 & \widetilde{\mathcal{K}}_{h,\tau}(\boldsymbol{\theta}^{10}) & 0 \\ 0 & 0 & 0 & \widetilde{\mathcal{K}}_{h,\tau}(\boldsymbol{\theta}^{01}) \end{pmatrix},$$

with the following blocks in the diagonal:

$$\widetilde{\mathcal{K}}_{h,\tau}(\boldsymbol{\theta}^{\alpha}) =$$

$$\frac{1}{2\tau} \begin{pmatrix} 2\widehat{B}_h(\boldsymbol{\theta}^{\alpha})+\tau\widehat{A}_h(\boldsymbol{\theta}^{\alpha}) & & \cdots & 0 \\ -2\widehat{B}_h(\boldsymbol{\theta}^{\alpha})+\tau\widehat{A}_h(\boldsymbol{\theta}^{\alpha}) \; 2\widehat{B}_h(\boldsymbol{\theta}^{\alpha})+\tau\widehat{A}_h(\boldsymbol{\theta}^{\alpha}) & & \cdots & 0 \\ \vdots & \ddots & \ddots & \vdots \\ 0 & \cdots & -2\widehat{B}_h(\boldsymbol{\theta}^{\alpha})+\tau\widehat{A}_h(\boldsymbol{\theta}^{\alpha}) \; 2\widehat{B}_h(\boldsymbol{\theta}^{\alpha})+\tau\widehat{A}_h(\boldsymbol{\theta}^{\alpha}) \end{pmatrix},$$

where $\alpha = \{(\alpha_1, \alpha_2)|\alpha_j \in \{0,1\}, j = 1, 2\}$. In a similar way, we can obtain the Fourier representation of the prolongation and restriction operators, that are $4M \times M$ and $M \times 4M$ matrices, respectively,

$$\widetilde{\mathcal{I}}_{2h}^{h}(\boldsymbol{\theta}) = \left(\widehat{I}_{2h}^{h}(\boldsymbol{\theta}^{00})I_M, \; \widehat{I}_{2h}^{h}(\boldsymbol{\theta}^{11})I_M, \; \widehat{I}_{2h}^{h}(\boldsymbol{\theta}^{10})I_M, \; \widehat{I}_{2h}^{h}(\boldsymbol{\theta}^{01})I_M \right)^T,$$

$$\widetilde{\mathcal{I}}_{h}^{2h}(\boldsymbol{\theta}) = \left(\widehat{I}_{h}^{2h}(\boldsymbol{\theta}^{00})I_M, \; \widehat{I}_{h}^{2h}(\boldsymbol{\theta}^{11})I_M, \; \widehat{I}_{h}^{2h}(\boldsymbol{\theta}^{10})I_M, \; \widehat{I}_{h}^{2h}(\boldsymbol{\theta}^{01})I_M \right).$$

Now, we are ready to perform the semi-algebraic two-grid analysis. We do this by combining the presented Fourier smoothing analysis and the Fourier analysis for the coarse-grid correction operator. The two-grid operator is defined as $\mathcal{T}_{h,\tau}^{2h} = \mathcal{S}_{h,\tau}^{\nu_2}\mathcal{C}_{h,\tau}^{2h}\mathcal{S}_{h,\tau}^{\nu_1}$, where, $\mathcal{S}_{h,\tau}$ is the smoothing operator such that the number of pre- and post-smoothing iterations are defined by ν_1 and ν_2, respectively, and $\mathcal{C}_{h,\tau}^{2h}$ is the coarse-grid correction operator.

The invariance property of the two-grid method comes from the invariance property of both components of this method. To be more precise, the coarse-grid correction operator, $\mathcal{C}_{h,\tau}^{2h}$, and the considered Gauss-Seidel smoothing operator, $\mathcal{S}_{h,\tau}$, both leave the space of $2h-$harmonics $\mathcal{F}_{2h}(\boldsymbol{\theta}^{00})$ invariant for an arbitrary Fourier frequency $\boldsymbol{\theta}^{00} \in \Theta_{2h}$.

Let us assume again that the error at the kth iteration is given by $\mathbf{c}_{\boldsymbol{\theta}}^{k}(t) \cdot \boldsymbol{\varphi}_h(\boldsymbol{\theta}, \cdot)^T$. By using the discretization of operators D_t and Σ_t we can obtain the relation $\widetilde{\mathcal{T}}_{h,\tau}^{2h}(\boldsymbol{\theta})\mathbf{c}_{\boldsymbol{\theta}}^{k}(t) \cdot \boldsymbol{\varphi}_h(\boldsymbol{\theta}, \cdot)^T$ that is the error after the application of the two-grid method, with $\widetilde{\mathcal{T}}_{h,\tau}^{2h}(\boldsymbol{\theta})$ a $4M \times 4M$ matrix, given by

$$\widetilde{\mathcal{T}}_{h,\tau}^{2h}(\boldsymbol{\theta}) = \widetilde{\mathcal{S}}_{h,\tau}^{\nu_2}(\boldsymbol{\theta}) \left(I_{4M} - \widetilde{\mathcal{I}}_{2h}^{h}(\boldsymbol{\theta}) \left(\widetilde{\mathcal{K}}_{2h,\tau}(\boldsymbol{\theta}) \right)^{-1} \widetilde{\mathcal{I}}_{h}^{2h}(\boldsymbol{\theta})\widetilde{\mathcal{K}}_{h,\tau}(\boldsymbol{\theta}) \right) \widetilde{\mathcal{S}}_{h,\tau}^{\nu_1}(\boldsymbol{\theta}).$$

By considering the Gauss-Seidel smoothing operator, the structure of matrix $\widetilde{\mathcal{S}}_{h,\tau}(\boldsymbol{\theta})$ is as follows

$$\widetilde{\mathcal{S}}_{h,\tau}(\boldsymbol{\theta}) = \begin{pmatrix} \widetilde{\mathcal{S}}_{h,\tau}(\boldsymbol{\theta}^{00}) & 0 & 0 & 0 \\ 0 & \widetilde{\mathcal{S}}_{h,\tau}(\boldsymbol{\theta}^{11}) & 0 & 0 \\ 0 & 0 & \widetilde{\mathcal{S}}_{h,\tau}(\boldsymbol{\theta}^{10}) & 0 \\ 0 & 0 & 0 & \widetilde{\mathcal{S}}_{h,\tau}(\boldsymbol{\theta}^{01}) \end{pmatrix},$$

where the matrix $\widetilde{\mathcal{S}}_{h,\tau}(\boldsymbol{\theta}^{\alpha})$, for $\alpha = \{(\alpha_1, \alpha_2)|\alpha_j \in \{0,1\}, j = 1,2\}$, has been previously described in detail. Finally, we can define the estimation of the two-grid convergence factor by the following expression:

$$\rho = \sup_{\boldsymbol{\theta} \in \Theta_{2h}} \left(\rho\left(\widetilde{\mathcal{T}}_{h,\tau}^{2h}(\boldsymbol{\theta}) \right) \right). \tag{2.8}$$

2.2. **SAMA results in two dimensions.** In this section we apply the SAMA analysis previously introduced to our model problem. We consider a bilinear finite element discretization on a uniform rectangular mesh to obtain the following discrete problem,

$$B_h \dot{\mathbf{u}}_h(t) + A_h \mathbf{u}_h(t) = F_h(t), \quad \mathbf{u}_h(0) = g_h, \quad t > 0.$$

When dealing with finite element discretizations of PDEs, the large sparse stiffness and mass matrices are typically built by the standard assembly procedure [8, 4, 6]. In the case of dealing with a structured grid, however, it suffices to represent the discrete operators by means of stencils [2]. The corresponding stencils obtained for the mass and stiffness matrices in two dimensions are as follows:

$$B_h = \frac{h^2}{36} \begin{bmatrix} 1 & 4 & 1 \\ 4 & 16 & 4 \\ 1 & 4 & 1 \end{bmatrix}, \qquad A_h = \frac{1}{3} \begin{bmatrix} -1 & -1 & -1 \\ -1 & 8 & -1 \\ -1 & -1 & -1 \end{bmatrix}.$$

To apply the presented analysis we also need to define the components of the multigrid waveform relaxation method. As we stated in the previous sections a Gauss-Seidel waveform relaxation is considered. Regarding the intergrid transfer operators, the stencil of the restriction operator, I_h^{2h}, is given by

$$I_h^{2h} = \frac{1}{16} \begin{bmatrix} 1 & 2 & 1 \\ 2 & 4 & 2 \\ 1 & 2 & 1 \end{bmatrix}.$$

The prolongation operator I_{2h}^h, is obtained according to the relation $I_h^{2h} = \frac{1}{4} I_{2h}^h$, see [10, 12] for more details.

In Figure 2, we show the obtained results by using the semi-algebraic mode analysis together with the experimentally computed convergence factors by W(1,1)-cycle. We analyze the convergence of the presented method depending on the parameter $\lambda = \tau/h^2$, which represents the anisotropy in the operator. As we can see in the left picture in Figure 2, the two-grid convergence factor for various values of parameter λ ranging from 2^{-12} to 2^{12} is bounded by 0.3117 when matrix B_h is considered as the mass matrix, as stated before. When we consider B_h as the identity matrix, however, the upper bound is 0.0695, see the right picture in Figure 2. One can see that the results when choosing B_h as the identity matrix match with the case in which the

applied discretization method is the finite difference scheme [7]. In this Figure, two smoothing steps are considered and the number of time steps are set to 32 ($M = 32$). We should notice that this two-grid analysis predicts the asymptotic convergence of the so-called W-cycle with two smoothing steps. Finally, we would like to mention that the asymptotic convergence factor of the proposed multigrid waveform relaxation is very satisfactory concerning the case where h is very small ($\tau = 10^{-5}$ and $\lambda = 2^{12}$), where the most iterative procedures lose out.

FIGURE 2. Two-grid convergence factors predicted by the SAMA together with the experimentally computed convergence factors by W(1,1)-cycle for various values of parameter $\lambda = \tau/h^2$. The matrix B_h is considered as the mass matrix and the identity matrix in the left and the right pictures, respectively.
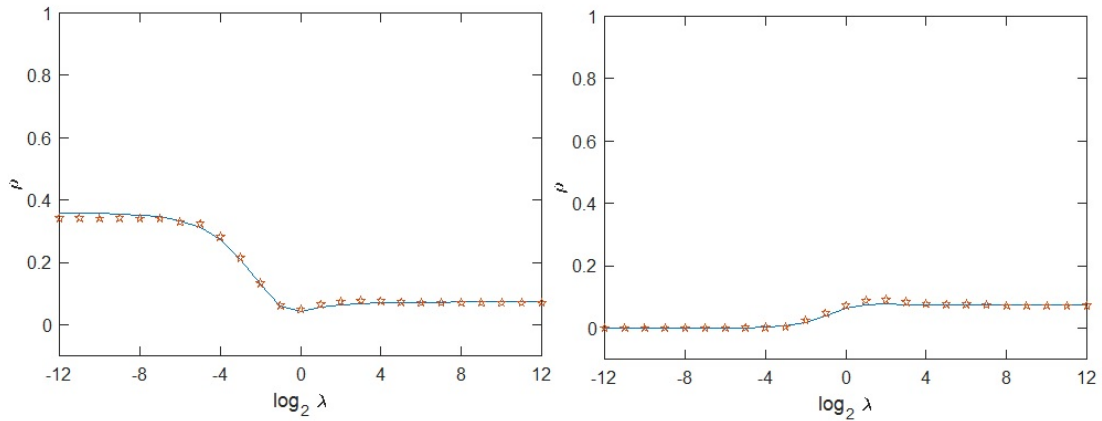
3. SAMA IN THREE DIMENSIONS

3.1. **Theoretical framework.** We have to do some changes on the analysis to extend the SAMA from two dimensions to three dimensions. As we did for the two dimensional case we need to define first the infinite grid $\mathcal{Q}_h$,

$$\mathcal{Q}_h = \{\mathbf{x} = \mathbf{k}h = (k_1 h_1, k_2 h_2, k_3 h_3), \ \mathbf{k} \in \mathbb{Z}^3\}.$$

In this case, the Fourier modes are $\varphi_h(\boldsymbol{\theta}, \mathbf{x}) = e^{i\boldsymbol{\theta}\cdot\mathbf{x}} = e^{i\theta_1 x_1} e^{i\theta_2 x_2} e^{i\theta_3 x_3}$ where $\boldsymbol{\theta} \in \Theta_h = (-\pi/h, \pi/h]^3$. As in the two dimensional case, any discrete grid function for a fixed t can be defined as a formal linear combination of Fourier modes . Also, we obtain a new 8−dimensional Fourier space generated by one low-frequency Fourier mode $\boldsymbol{\theta} = \boldsymbol{\theta}^{000} \in \Theta_{2h} = (-\pi/2h, \pi/2h]^3$ as follows:

$$\mathcal{F}_{2h}(\boldsymbol{\theta}) = \text{span}\{\varphi_h(\boldsymbol{\theta}^{000}, \cdot), \varphi_h(\boldsymbol{\theta}^{111}, \cdot), \varphi_h(\boldsymbol{\theta}^{100}, \cdot),$$
$$\varphi_h(\boldsymbol{\theta}^{011}, \cdot), \varphi_h(\boldsymbol{\theta}^{010}, \cdot), \varphi_h(\boldsymbol{\theta}^{101}, \cdot), \varphi_h(\boldsymbol{\theta}^{001}, \cdot), \varphi_h(\boldsymbol{\theta}^{110}, \cdot)\},$$

such that the high-frequencies are given by the following equation

$$\boldsymbol{\theta}^{\alpha} = \boldsymbol{\theta}^{000} - (\,\alpha_1\mathrm{sign}(\theta_1), \alpha_2\mathrm{sign}(\theta_2), \alpha_3\mathrm{sign}(\theta_3)\,)\,\frac{\pi}{h},$$

where, $\boldsymbol{\theta}^{000} = (\theta_1, \theta_2, \theta_3)$ and $\alpha = \{(\alpha_1, \alpha_2, \alpha_3)\,|\,\alpha_j \in \{0,1\}, j = 1, 2, 3\}$.

By the above definitions the resulting Fourier representations of the smoothing, coarse-grid correction and two-grid operators are $8M \times 8M$ matrices that can be computed following the same idea carried out in Section 2.1 for the two dimensional case. So in fact, SAMA in three dimensions is based on a three dimensional spatial LFA combined with an exact analysis in the time variable.

3.2. SAMA results in three dimensions.
Here we consider the discretization of our model problem by using trilinear finite elements. Similarly to the two dimensional case, first we define the stencil forms of the mass and stiffness matrices. By some computations we can obtain the stencils for B_h and A_h in three dimensions as follows:

$$B_h = \frac{h^3}{216}\left[\begin{bmatrix} 1 & 4 & 1 \\ 4 & 16 & 4 \\ 1 & 4 & 1 \end{bmatrix} \begin{bmatrix} 4 & 16 & 4 \\ 16 & 64 & 16 \\ 4 & 16 & 4 \end{bmatrix} \begin{bmatrix} 1 & 4 & 1 \\ 4 & 16 & 4 \\ 1 & 4 & 1 \end{bmatrix} \right],$$

$$A_h = \frac{h}{12}\left[\begin{bmatrix} -1 & -2 & -1 \\ -2 & 0 & -2 \\ -1 & -2 & -1 \end{bmatrix} \begin{bmatrix} -2 & 0 & -2 \\ 0 & 32 & 0 \\ -2 & 0 & -2 \end{bmatrix} \begin{bmatrix} -1 & -2 & -1 \\ -2 & 0 & -2 \\ -1 & -2 & -1 \end{bmatrix} \right].$$

Also, we need to fix the multigrid components. As before, we use a Gauss-Seidel waveform relaxation and the inter-grid transfer operators are given as follows. The stencil of the restriction operator, I_h^{2h}, is,

$$I_h^{2h} = \frac{1}{64}\left[\begin{bmatrix} 1 & 2 & 1 \\ 2 & 4 & 2 \\ 1 & 2 & 1 \end{bmatrix} \begin{bmatrix} 2 & 4 & 2 \\ 4 & 8 & 4 \\ 2 & 4 & 2 \end{bmatrix} \begin{bmatrix} 1 & 2 & 1 \\ 2 & 4 & 2 \\ 1 & 2 & 1 \end{bmatrix} \right],$$

and the prolongation operator I_{2h}^{h} will satisfy $I_h^{2h} = \frac{1}{8}I_{2h}^{h}$. In Figure 3, we show the obtained results by two-grid SAMA analysis in three dimensions together with the experimentally computed convergence factors by W(1,1)-cycle. As in the two dimensional case, we analyze the convergence of the presented method accordingly to parameter $\lambda = \tau/h^2$ (which denotes the anisotropy in the operator). We consider again two different cases: when B_h is the mass matrix (left picture) and when B_h is assumed to be the identity matrix (right picture). Here we obtain very similar results to the two dimensional case. To be more precise, when matrix B_h is the identity matrix, the results match very good with the case in which a finite difference discretization method is used. As we expected, the upper bound for the predicted convergence factor slightly increases for both cases being equal to 0.4040 and 0.0881 when B_h is the mass matrix and identity matrix, respectively. The results are presented for two smoothing steps and $M = 32$. Moreover as expected, the asymptotic convergence factor of the proposed multigrid waveform relaxation is very satisfactory concerning the case where h tends to be very small.

FIGURE 3. Two-grid convergence factors predicted by the SAMA together with the experimentally computed convergence factors by W(1,1)-cycle for various values of parameter $\lambda = \tau/h^2$. Matrix B_h is considered as the mass matrix and the identity matrix in the left and the right pictures, respectively.
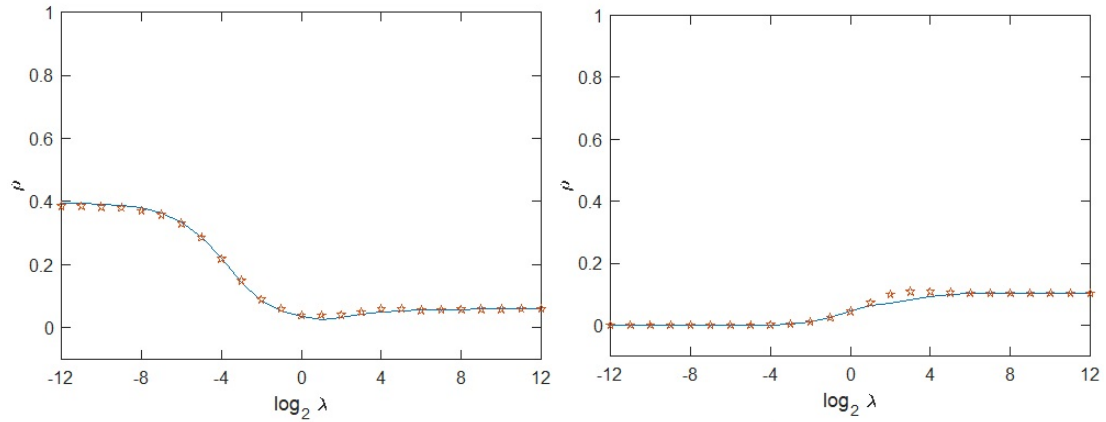
4. CONCLUSIONS

In this work, we presented the two-grid SAMA analysis for predicting the convergence factor of a multigrid waveform relaxation method for finite element discretizations in two and three spatial dimensions. We considered the Crank-Nicolson discretization in time and bilinear and trilinear finite element methods for the spatial discretization in two and three dimensions, respectively. The presented results when matrix B_h is the identity matrix, are comparable with the case in which a finite difference discretization method is used. The proposed SAMA analysis allows us to systematically study the behavior of the multigrid waveform relaxation method for finite element discretizations.

REFERENCES

[1] A. Brandt, *Multigrid solvers for non-elliptic and singular-perturbation steady-state problems*, The Weizmann Institute of Science, Rehovot, Israel, 1981.

[2] C. Engwer, RD. Falgout, and UM. Yang, *Stencil computations for PDEbased applications with examples from DUNE and hypre*. Concurrency and Computation: Practice and Experience, *29* 17 (2017), e4097.

[3] S. Friedhoff and S. MacLachlan, *A generalized predictive analysis tool for multigrid methods*, Numerical Linear Algebra with Applications, *22*(4) (2015), 618–647, Doi: 10.1002/nla.1977

[4] G. Karakoc, S. Battal, S. Kumar Bhowmik, and F. Gao, *A numerical study using finite element method for generalized Rosenau-Kawahara-RLW equation*. Computational Methods for Differ. Equ., *7*(3) (2019), 319–333.

[5] M. J. Gander, *50 years of time parallel time integration: In Multiple Shooting and Time Domain Decomposition Methods*, Springer, Cham *69-113*, 2015.

[6] M. Dehghan, B. N. Saray, and M. Lakestani, *Three methods based on the interpolation scaling functions and the mixed collocation finite difference schemes for the numerical solution of the*

nonlinear generalized BurgersHuxley equation, Mathematical and Computer Modelling, *55*(3-4) (2012), 1129–1142.

[7] F. J. Gaspar and C. Rodrigo, *Multigrid waveform relaxation for the time-fractional heat equation*, SIAM Journal on Scientific Computing, *39*(4) (2017), A1201–A1224, Doi: 10.1137/16M1090193

[8] M. S. Gockenbach, *Understanding and implementing the finite element method*, SIAM, *97*, 2006.

[9] C. Lubich and A. Ostermann, *Multi-grid dynamic iteration for parabolic equations*, BIT Numerical Mathematics, *27*(2), 216–234.

[10] U. Trottenberg, C. W. Oosterlee, and A. Schuller, *Multigrid*, Elsevier, 2000.

[11] S. Vandewalle and D. Roose, *The parallel waveform relaxation multigrid method*, Parallel Processing for Scientific Computing, 152–156, 1989.

[12] R. Wienands and W. Joppich, *Practical Fourier analysis for multigrid methods*, Chapman and Hall/CRC, 2004.